Electronic Supplementary Material (ESI) for Journal of Materials Chemistry B.

Supporting Information

Facile synthesis of $Au@Mn_3O_4$ magneto-plasmonic nanoflowers for T_1-weighted magnetic resonance imaging and photothermal therapy of cancer

Gohar Ijaz Dar[a,b], M. Zubair Iqbal[a,c*], Ozioma Udochukwu Akakuru[a,b], Chenyang Yao[a,b], Gul Awiaz[a,b], Aiguo Wu[a*]

[a]Cixi Institute of Biomedical Engineering, CAS Key Laboratory of Magnetic Materials and Devices, & Key Laboratory of Additive Manufacturing Materials of Zhejiang Province, Ningbo Institute of Materials Technology and Engineering, Chinese Academy of Sciences, Ningbo 315201, P.R. China

[b]University of Chinese Academy of Sciences, No.19(A) Yuquan Road, Shijingshan District, Beijing, 100049, P.R. China

[c]School of Materials Science and Engineering, Zhejiang Sci-Tech University, No. 2 Road of Xiasha, Hangzhou, 310018, PR China.

**Corresponding author email: aiguo@nimte.ac.cn, zubair@nimte.ac.cn*
Tel: +86 574 87617278; Fax: +86-57486685163

Experimental section

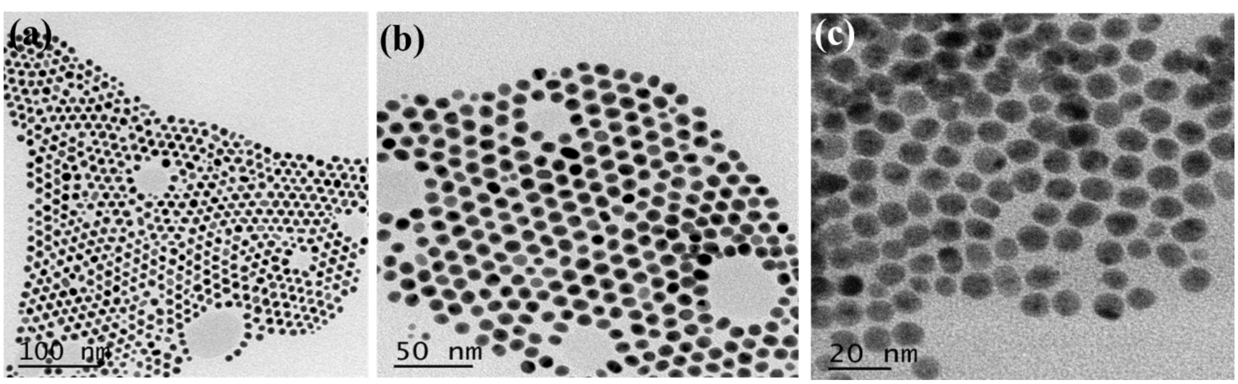

Figure S1. TEM images of monodisperse Au nanoparticles at various magnifications. (a) scale bar 100 nm. (b) scale bare 50 nm and (c) scale bar 20 nm.

Synthesis process of NFs with 30 min, 1h, and 1.5 h

In the synthesis of $Au@Mn_3O_4$ nanoflowers experiments were also conducted at various times like 30 min, 60 min, 90 min, and 120 min. The TEM images of the 30 min, 60 min, and 90 min were shown in Figure S2. The temperature of all the systems remains constants (315 °C).

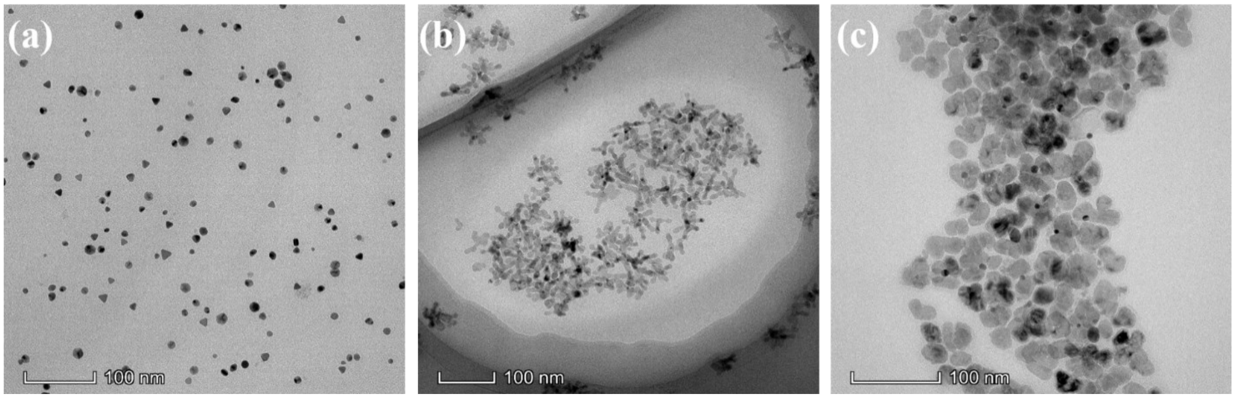

Figure S2. TEM images of various results experienced at different intervals of time. (a) TEM image shows the 30 min time interval (scale bar =100 nm). (b) The TEM image of reaction time was 60 min (scale bar = 100 nm). (c) TEM image of reaction at 90 min (scale bar =100 nm).

Characterization

DLS and Zeta Potential of Au@Mn_3O_4@PF-127

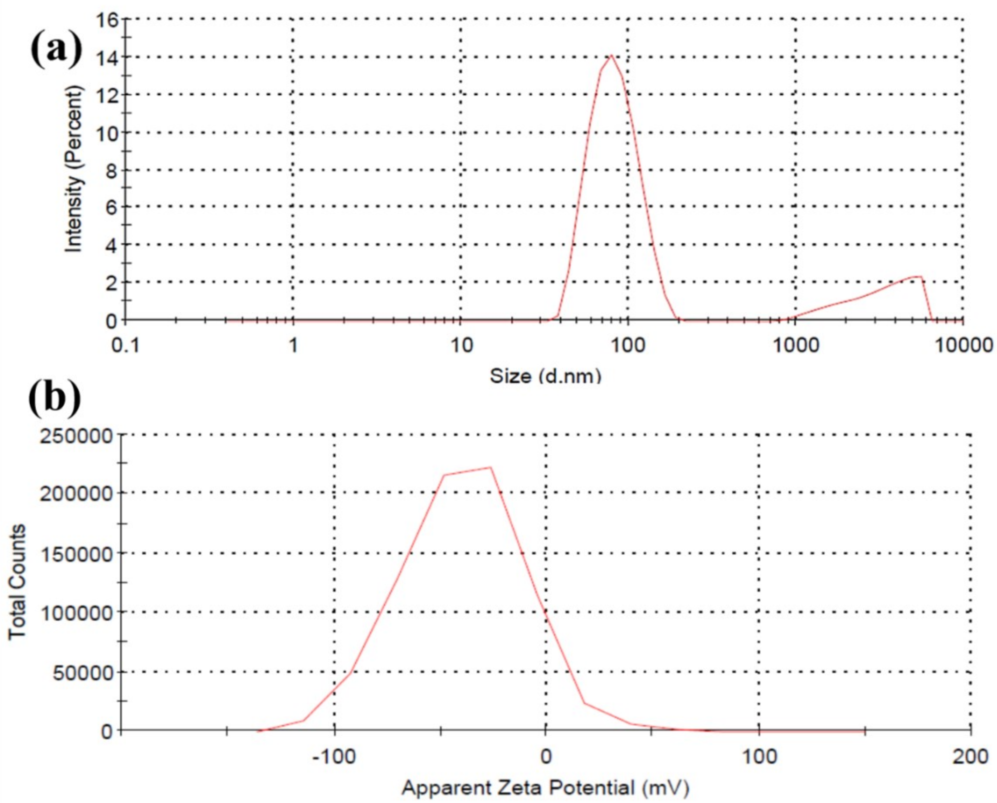

Figure S3. Dynamic light scattering and Zeta potential results. (a) DLS distribution of prepare Au@Mn_3O_4@PF-127 nanoflowers. (b) Zeta Potential of synthesized NFs @ PF-127.

The magnitude of the zeta potential is predictive of colloidal stability. Nanoparticles with Zeta Potential values greater than +25 mV or less than -25 mV typically have high degrees of stability [1]. As per our observation of the prepared NFs, the zeta potential was measure at -39.6 mV. It shows that the prepared nanoflowers are potentially stable in the suspension and it is a positive factor for biomedical applications.

Table S1. Relaxivity Data of Manganese Oxide-Based Nanoparticles

Name	**Core Material**	**r_1 ($mM^{-1}S^{-1}$)**	**B_0 (T)**	**Ref.**
Au@Mn_3O_4 NFs	Mn_3O_4	5.74	0.55	This Work
HMONs	MnO	2.58	7	[2]
MnO	MnO	0.12	3	[3]
HMnO@mSiO_2	MnO	1.72	1.5	[4]
Mn_3O_4 nanocubes	Mn_3O_4	1.08	3	[5]
Mn_3O_4 nanospheres	Mn_3O_4	1.31	3	
Mn_3O_4 nanoplates	Mn_3O_4	2.06	3	
Mn-MSNs	MnO(Mn_3O_4)/SiO_2	2.28	3	[6]
Spherical Mn_3O_4	Mn_3O_4	2.38	1.5	[7]
HSA-MONP	MnO	1.97	7	[8]
HMONs	Mn_3O_4	1.42	3	[9]
Mn_3O_4@SiO_2	Mn_3O_4	0.47	3	[10]
Fe_3O_4/MnO hybrid	Fe_3O_4/MnO	1.4	3	[11]

Nanoparticle annotations: NFs- nanoflowers, HMONs-hollow manganese oxide nanoparticles, HMnO@mSiO_2-mesoporous silica-coated hollow MnO nanoparticles, HAS-MNOP-human serum albumin-coated manganese oxide nanoparticles,

PTT efficiency of the Au@Mn_3O_4@PF-127 NFs

The photothermal conversion effect of the prepared Au@Mn_3O_4@PF-127 NFs was measured through the implementation of the reported method [12, 13]. The prepared sample (150µg/ml) was placed in the Macro plastic cuvette and irradiated by 808 nm laser (1.2 W/cm^2) for 10 min interval. The water sample was considered as a control. Then, the photothermal conversion efficiency of prepared nanoflowers was calculated as follows:

The total input heat energy and dissipation of the system is expressed as in equation

$$\sum_i m_i C_{p,i} \frac{dT}{dt} = Q_{NPs} + Q_s - Q_{loss} \qquad (1)$$

Where, the suffix "*i*" of *m* and *Cp* refers to solvent (water) or dispersed matter (nanoparticles). C*p* and *m* are the heat capacity and mass respectively. T is referred to as temperature of solution and Q_{NPs} is the heat energy from the prepared nanoflowers, Q_s is referred to as heat energy by sample cell and Q_{loss} is the heat dissipated by the system in the surroundings by air. The Q_{NPs} can be obtained from the following equation (2)

$$Q_{NPs} = I\,(1\text{-}10^{-A\lambda})\ \eta \qquad (2)$$

Where '*I*' referred to as the laser power density, 'Aλ' is the absorbance of the $Au@Mn_3O_4@PF$-127 NFs against the 808 nm wavelength and 'η' is heat energy conversion by the prepared $Au@Mn_3O_4@PF$-127 NFs in aqueous solution.

Q_{loss} in equation (1) is the loss of heat energy in the surroundings by air and can be expressed as:

$$Q_{loss} = hA\Delta T = hs(T\text{-}T_{surr}) \qquad (3)$$

As 'h' is the heat transfer coefficient, 'A' is referred to as the surface area of the cuvette, 'T' is the solution temperature and 'T_{surr}' is the atmosphere surrounding temperature. As [$\Delta T_{max,\ mix} = T_{max} - T_{surr}$].

Qs in equation (1) is the heat energy-related to the energy absorbed by the sample cell without NFs, so the heat input and dissipation is equal. Therefore, the equation can be written as:

$$Q_s + Q_{NPs} = Q_{loss} = hA\,(T_{max} - T_{surr}) \qquad (4)$$

Rendering to the temperature profile as shown in Figure 4a, the [$\Delta T_{max,\ mix} = T_{max} - T_{surr}$] was ~ 40 °C for 150 μg/ml.

According to the above equations (2), (3), and (4), the heat energy conversion efficiency can be written as:

$$\eta = \frac{hA(\Delta T_{max,mix} - \Delta T_{max,\,water})}{I(1 - 10^{-A\lambda})} \qquad (5)$$

As in the equation (5) the ‘hA' is unknown and the θ will introduce to calculate the value of hA. As θ is equal to $\Delta T / \Delta T_{max}$. By the substituting the value of θ into equation 1, the equation will become

$$\frac{d\theta}{dt} = \frac{hA}{\sum_i m_i C_{p,i}} [\frac{Q_{NP_s} + Q_s}{hA\Delta T_{max}} - \theta] \quad (6)$$

when the laser light is being turned off then the $Q_s + Q_{NPs}$ is equal to zero and the equation becomes

$$dt = -\frac{\sum_i m_i C_{p,i}}{hA} \frac{d\theta}{\theta} \quad (7)$$

Calculating the $\frac{\sum_i m_i C_{p,i}}{hA}$ by the linear time data against –ln(θ) and then integrating the equation (7). The ‘m’ and ‘C’ is the mass (0.2 g) and the specific heat capacity of the deionized water (4.2 J/g) employed as solvent. Subsequently, the value of ‘hA' is calculated as 0.0280. Generally, the specific heat value of the deionized water is much larger than other materials, so the values of m_{NPs} and $C_{p,NPs}$ were neglected. The laser power intensity was 2.99 W, the $A\lambda$ was calculated as 1.6. By substituting the all values in the equation (5), the photothermal conversion efficiency ‘η’ of the prepared $Au@Mn_3O_4@PF$-127 NFs is calculated as ~ 38% which is much better and higher than other reported composite materials.

Table S2. Comparison of photothermal conversion efficiency of various Au other nanocomposites.

Materials	Wavelength Irradiation (nm)	Laser Power (W)	Efficiency (%)	Ref
$Au@Mn_3O_4@PF$-127 NFs	808	1.2 W/cm^2	38	Present work
Biodegradable Au nano vesicles	808	1	37	[14]
FePt NPs	800	1µJ / Pulse	30	[15]

Au / SiO_2 nano shells	815	0.163	34	[16]
Au nano rods	808	1	22	[14]
Au nano shells	808	2	25	[17]
Cu_9S_5 NPs	980	0.51	25.7	[18]
HER-DIR-SPIO-PLGA/PFP NPs	808	2	5.9	[19]
$Cu_{2-x}Se$ NPs	800	2	22	[20]
Au-Fe_2C JNPs	808	1	30.2	[21]
Cys-Cus NPs	980	0.288	21.3	[22]

References

1 J. D. Clogston and A. K. Patri, in *Characterization of nanoparticles intended for drug delivery*, Springer, 2011, pp. 63-70.

2 B. Y. W. Hsu, M. Ng, Y. Zhang, S. Y. Wong, K. Bhakoo, X. Li and J. Wang, *Advanced Functional Materials*, 2015, **25**, 5269-5276.

3 A. A. Gilad, P. Walczak, M. T. McMahon, H. B. Na, J. H. Lee, K. An, T. Hyeon, P. C. M. van Zijl and J. W. M. Bulte, *Magnetic Resonance in Medicine*, 2008, **60**, 1-7.

4 T. Kim, E. Momin, J. Choi, K. Yuan, H. Zaidi, J. Kim, M. Park, N. Lee, M. T. McMahon, A. Quinones-Hinojosa, J. W. Bulte, T. Hyeon and A. A. Gilad, *Journal of the American Chemical Society*, 2011, **133**, 2955-2961.

5 C.-C. Huang, N.-H. Khu and C.-S. Yeh, *Biomaterials*, 2010, **31**, 4073-4078.

6 Y. Chen, H. Chen, S. Zhang, F. Chen, S. Sun, Q. He, M. Ma, X. Wang, H. Wu, L. Zhang, L. Zhang and J. Shi, *Biomaterials*, 2012, **33**, 2388-2398.

7 K. An, M. Park, J. H. Yu, H. B. Na, N. Lee, J. Park, S. H. Choi, I. C. Song, W. K. Moon and T. Hyeon, *European Journal of Inorganic Chemistry*, 2012, **2012**, 2148-2155.

8 T. D. Schladt, K. Schneider, M. I. Shukoor, F. Natalio, H. Bauer, M. N. Tahir, S. Weber, L. M. Schreiber, H. C. Schroder, W. E. G. Muller and W. Tremel, *Journal of Materials Chemistry*, 2010, **20**, 8297-8304.

9 J. Shin, R. M. Anisur, M. K. Ko, G. H. Im, J. H. Lee and I. S. Lee, *Angewandte Chemie International Edition*, 2009, **48**, 321-324.

10 H. Yang, Y. Zhuang, H. Hu, X. Du, C. Zhang, X. Shi, H. Wu and S. Yang, *Advanced Functional Materials*, 2010, **20**, 1733-1741.

11 G. H. Im, S. M. Kim, D. G. Lee, W. J. Lee, J. H. Lee and I. S. Lee, *Biomaterials*, 2013, **34**, 2069-2076.

12 Y. Liu, K. Ai, J. Liu, M. Deng, Y. He and L. J. A. m. Lu, 2013, **25**, 1353-1359.

13 J. Zhou, Z. Lu, X. Zhu, X. Wang, Y. Liao, Z. Ma and F. J. B. Li, 2013, **34**, 9584-9592.

14 P. Huang, J. Lin, W. Li, P. Rong, Z. Wang, S. Wang, X. Wang, X. Sun, M. Aronova and G. J. A. C. I. E. Niu, 2013, **52**, 13958-13964.

15 C.-L. Chen, L.-R. Kuo, S.-Y. Lee, Y.-K. Hwu, S.-W. Chou, C.-C. Chen, F.-H. Chang, K.-H. Lin, D.-H. Tsai and Y.-Y. J. B. Chen, 2013, **34**, 1128-1134.

16 J. R. Cole, N. A. Mirin, M. W. Knight, G. P. Goodrich and N. J. J. T. J. o. P. C. C. Halas, 2009, **113**, 12090-12094.

17 V. P. Pattani, J. W. J. L. i. s. Tunnell and medicine, 2012, **44**, 675-684.

18 Q. Tian, F. Jiang, R. Zou, Q. Liu, Z. Chen, M. Zhu, S. Yang, J. Wang, J. Wang and J. J. A. n. Hu, 2011, **5**, 9761-9771.

19 L. Deng, X. Cai, D. Sheng, Y. Yang, E. M. Strohm, Z. Wang, H. Ran, D. Wang, Y. Zheng and P. J. T. Li, 2017, **7**, 4410.

20 C. M. Hessel, V. P. Pattani, M. Rasch, M. G. Panthani, B. Koo, J. W. Tunnell and B. A. J. N. l. Korgel, 2011, **11**, 2560-2566.

21 Y. Ju, H. Zhang, J. Yu, S. Tong, N. Tian, Z. Wang, X. Wang, X. Su, X. Chu and J. J. A. n. Lin, 2017, **11**, 9239-9248.

22 X. Liu, B. Li, F. Fu, K. Xu, R. Zou, Q. Wang, B. Zhang, Z. Chen and J. J. D. t. Hu, 2014, **43**, 11709-11715.